

Catalogue of observed tangents to the spiral arms in the Milky Way galaxy

Jacques P. Vallée

National Research Council Canada, National Science Infrastructure portfolio, Herzberg
Astrophysics, 5071 West Saanich Road, Victoria, B.C., Canada V9E 2E7

Keywords: Galaxy: disk - Galaxy: structure – Galaxy: fundamental parameters –
ISM: kinematics and dynamics

Accepted: 2014 August 23; to appear in the *Astrophysical Journal Suppl. Ser.* (2014 Oct. issue)

Abstract. From the Sun's location in the Galactic disk, one can use different arm tracers (CO, HI, thermal or ionized or relativistic electrons, masers, cold and hot dust, etc) to locate a tangent to each spiral arm in the disk of the Milky Way. We present a master Catalogue of the astronomically observed tangents to the Galaxy's spiral arms, using different arm tracers from the literature. Some arm tracers can have slightly divergent results from several papers, so a mean value is taken – see Appendix for CO, HII, and masers. The Catalogue of means currently consists of 63 mean tracer entries, spread over many arms (Carina, Crux-Centaurus, Norma, Perseus origin, near 3-kpc, Scutum, Sagittarius), stemming from 107 original arm tracer entries.

Additionally, we updated and revised a previous statistical analysis of the angular offset and linear separation from the mid-arm, for each different mean arm tracer. Given enough arm tracers, and summing and averaging over all four spiral arms, one could determine if arm tracers have separate and parallel lanes in the Milky Way. This statistical analysis allows a cross-cut of a galactic spiral arm to be made, confirming a recent discovery of a linear separation between arm tracers. Here, from the mid-arm's CO to the inner edge's hot dust, the arm halfwidth is about 340 pc; doubling would yield a full arm width of 680 pc. We briefly compare these observations with the predictions of many spiral arm theories, notably the density-wave theory.

1. Introduction

Our whole Galaxy is composed of a disk orbiting around a nuclear bulge, all happening within a dark halo. At a distance between 7.5 and 8.5 kpc from the Galactic Center, the Sun is immersed inside the galactic disk, composed mainly of stars with the addition of dust (warm and hot), gas (molecular and atomic), ionized gas and thermal electrons, cosmic rays and relativistic electrons, and magnetic fields. For a review of some physical properties (density, temperature, etc) of the gas phases and the magnetic fields in the interstellar medium, see Heiles & Haverkorn (2012). Near the Galactic Center, there are two coexisting bar-like structures pointed between 14° to 45° with respect to the line of sight of the Sun to the Galactic Center, a stellar bulge, and the usual black hole at the center (Green et al 2011 – fig.5). The majority of published papers favors a 4-arm spiral model in the galactic disk. There is still a bit of controversy left, as one-sixth of all recent publications favor a 2-arm spiral structure (see Vallée 2014b).

Here our interest lies in the disk. Massive stars, and a large number of less massive stars, molecular gas and dust are preferentially located in spiral arms. In the Milky Way, a spiral arm has a mean pitch angle near 12° , although estimates vary slightly. Previous sketches of the Milky Way galaxy showed stellar arms arranged in a spiral form, without much details across the arms. Recently, more details have become available.

The Sun is located in the interarm region (**Figure 1**), between the Perseus arm and the Sagittarius arm. There is a local “armlet” (not shown here) of length about 2.2 kpc at a galactic longitude near 77° (e.g., section 9 in Vallée 2011). There is no ‘molecular ring’ near the Galactic Center, but a molecular region encompassing the origins of the four spiral arms (Section 3.2 in Vallée 2008; Dobbs & Burkert 2012). The “Perseus origin arm” near the Galactic Center (Figure 1) is at times referred to as the “far 3-kpc arm” (e.g., Dame & Thaddeus 2008 and 2011, their -23° arm at 337° ; table 3 in García et al 2014). The “Crux” arm is often called the “Centaurus” arm. The “Cygnus” arm is often called the “outer” arm. The “Cygnus + I” arm is the continuation of the Scutum arm (Dame & Thaddeus – Fig.4). In Figure 1 a single bar is sketched (but no bulge), since the position angle of both bars are still loosely defined or explained (Martinez-Valpuesta 2013, their Fig.1; Romero-Gómez et al 2013, their fig.1). We know from the measured line-of-sight velocities at longitude $l=0^\circ$ that the near 3-kpc arm is expanding at -50 km/s (close to the origin of the Norma arm), and that the far 3-kpc arm is expanding at $+50$ km/s (close to the start of the Sagittarius arm). The author is not aware of any similar velocity measurement close to the start of the ‘Perseus origin’ arm, nor of the start of the Scutum arm.

There have been numerous published results for the spiral arms of the Milky Way. With the Sun in the Milky Way disk, the majority of published observational results have focused on small, different parts of our Galaxy, using different arm tracers, listing the arm shape (logarithmic or wavy or polynomial), the arm pitch angle (from the circular tangent), the number of arms (2 or 4 or 6), and the interarm separation through the Sun (around 3 kpc). Given conflicting results over time, statistics on arm parameters were done for the period 1980-onward, catalogued in blocks of 15 to 20 each (for the blocks, see Vallée 1995, 2002, 2005, 2008, 2013, 2014a, 2014b). A composite map of all these small-scale views could approximate the mid-scale view – see Figure 1.

Small tables of arm tangents have been published before. Table 1 in Englmaier & Gerhard (1999) had 32 entries of tracer tangents, but none for the Carina arm near 284° , their ‘inner Galaxy’ column mixed together the Scutum arm and the inner 3-kpc arm, and their far ‘3-kpc’ arm near -21° is now called the ‘Perseus origin’ arm. Table 2 in Vallée (2008) had 39 tracer entries, Table 1 in Vallée (2012) had 12 tracer entries, while Table 3 in Vallée (2014a) had 43 tracer entries.

Here we embarked on an extensive literature review, to glean more arm tangents from different tracers. We recorded the complete published reference of each tracer (journal, table, figure, section), and thus were able to delete or replace erroneous or misplaced references. Also, newer instrumentation allows the detection of the arm tangents as inferred from the recent 6.7 GHz methanol maser or water maser data. The master catalogue of published galactic longitudes of arm tangents is given in **Table 1**. In Table 1, an arm is defined and labeled in only one Galactic Quadrant (I or IV); its continuation in another quadrant has another name, and we listed 63 different entries of the means of different tracer tangents (one specific tracer entry per arm), about half more than in Vallée (2014a). As much as 17 of these 63 different entries are themselves a mean of two or more published values. In addition, in **Appendix A**, we provided 38 individual CO entries (Table 3), 13 individual HII entries (Table 4), and 10 individual maser entries (Table 5). Thus, all in all, we catalogued 107 different tracer entries over these four tables ($63 - 17 + 38 + 13 + 10$). For the Centaurux-Crux arm, the CO arm tangent was originally given as 310° by Bronfman et al (1988 – fig.7), then appeared as a typo as 300° in Bronfman (1992 – his Fig.6), and was later given as 309° in Garcia et al (2014 – their Fig. 14); in Appendix A we entered only the original value of 310° from the first publication in 1988.

We provide here a short CO analysis of the published results. The Columbia CO Surveys made at low angular resolution (~ 8 arcmin) of the low excitation ($J=1-0$), low temperature (~ 10 K), ^{12}CO tracer (emitting at 115 GHz), as integrated over a velocity range associated with a spiral arm, is useful to indicate the middle of the arm. For the Carina arm, the CO tracer is given in the literature with a longitude varying from 280° to 283° , depending on the different mathematical analyses done. The different CO analyses gave slightly different output values from roughly the same observed data, especially when using different averaging bin sizes in galactic longitudes (asymmetric amplitude with galactic longitude), or using different input data cutoff (63% removal, representing the disk emission with longitude – see Fig. 14 in García et al 2014), or using a simple or complex disk emission model (Section 2 in Bronfman 1992). Of all the CO tracers used as arm tangents, the longitude-velocity analysis of García et al (2014) gave the largest longitude values for the Crux-Centaurus arm, Norma arm, and Perseus Origin (3-kpc) arm (their Table 3). They noted that their arms were first defined and delineated in the longitude-velocity diagram (their Fig. 9), and later transposed and averaged in the longitude-distance diagram. Such an analysis is bound to use somewhat arbitrary boundaries in the longitude-velocity diagram (removing some reassigned arm clouds), and the arm tangent obtained later in the other diagram with the transposed clouds could have a bigger error bar. The low resolution ($8''$) Columbia CO survey (linked to the mid-arm) does differ as it should from the high resolution ($50''$) Stoney Brook survey of warm CO cores (linked to new star forming regions - Solomon et al 1985).

Table 1 – Catalogue of published different spiral arm tracers (since 1980), with only one mean tracer value for each arm

Arm Name	Chemical tracer	Gal. longit. of arm tangent ⁽¹⁾	Ang. dist. ⁽²⁾ to ¹² CO	Linear separation inside arm ⁽³⁾ from ¹² CO	References ⁽⁴⁾
Carina	¹² CO at 8'	282°	0°	0 pc, at 5 kpc ⁽³⁾	Bronfman et al (2000b – table 2); see Table 3
	Thermal electron	283°	1°	87 pc	Taylor & Cordes (1993 – fig.4)
	HII complex	284°	2°	174 pc	Russeil (2003 – table 6); see Table 4
	Dust 240µm	284°	2°	174 pc	Drimmel (2000 –fig.1)
	Dust 60µm	285°	3°	262 pc	Bloemen et al (1990 – fig.5)
	FIR [CII] & [NII]	287°	5°	435 pc	Steiman-Cameron et al (2010 – sect. 2.1)
Crux-Centaurus	¹² CO at 8'	309°	0°	0 pc, at 6 kpc ⁽³⁾	Bronfman et al (2000b – table 2); see Table 3
	Thermal electron	309°	0°	0 pc	Taylor & Cordes (1993 – fig.4)
	HII complex	309°	0°	0 pc	Russeil (2003 – table 6); see Table 4
	FIR [CII] & [NII]	309°	0°	0 pc	Steiman-Cameron et al (2010 – sect. 2.1)
	HI atom	310°	1°	105 pc	Englmaier & Gerhard (1999- table 1)
	²⁶ Al	310°	1°	105 pc	Chen et al (1996- fig.1)
	Sync. 408 MHz	310°	1°	105 pc	Beuermann et al (1985 – fig.1)
	Dust 240µm	311°	2°	209 pc	Drimmel (2000 – fig. 1)
	Dust 60µm	311°	2°	209 pc	Bloemen et al (1990 – fig.5)
	Dust 870µm	311°	2°	209 pc	Beuther et al (2012 – fig.2; another peak at 305°)
Norma	HII complex	325°	-3°	-366 pc	Downes et al (1980 – fig.4); see Table 4
	²⁶ Al	325°	-3°	-366 pc	Chen et al (1996 – fig.1)
	¹² CO at 8'	328°	0°	0 pc, at 7 kpc ⁽³⁾	Bronfman et al (2000b – table 2); see Table 3
	Thermal electron	328°	0°	0 pc	Taylor & Cordes (1993 – fig.4)
	HI atom	328°	0°	0 pc	Englmaier & Gerhard (1999 – table 1)
	Sync. 408 MHz	328°	0°	0 pc	Beuermann et al (1985 – fig.1)
	Dust 60µm	329°	1°	122 pc	Bloemen et al (1990 – fig.5)
	Methanol masers	331.5°	3.5°	427 pc	Caswell et al (2011 – sect. 4.6.2); see Table 5
	Dust 240µm	332°	4°	488 pc	Drimmel (2000 – fig. 1)
	Dust 2.4µm	332°	4°	488 pc	Hayakawa et al (1981 – fig.2a)
Dust 870µm	332°	4°	488 pc	Beuther et al (2012 – fig.3)	
Start of Perseus	¹² CO at 8'	337°	0°	0 pc, at 8 kpc ⁽³⁾	Bronfman et al (2000b – table 2); see Table 3
	FIR [CII] & [NII]	338°	1°	140 pc	Steiman-Cameron et al (2010 – sect. 2.1)
	Dust 870µm	338°	1°	140 pc	Beuther et al (2012 – fig.3)
	Methanol masers	338°	1°	140 pc	Green et al (2011 – sect. 3.3.1); see Table 5
	Sync. 408 MHz	339°	2°	279 pc	Beuermann et al (1985 – fig.1)
	Dust 2.4µm	339°	2°	279 pc	Hayakawa et al (1981 – fig.2a)
	Dust 60µm	340°	3°	419 pc	Bloemen et al (1990 – fig.5)
Near 3-kpc Arm	¹² CO at 8'	026°	0°	0 pc, at 6 kpc ⁽³⁾	Cohen et al (1980 – fig.3); see Table 3
	HII complex	025°	1°	105 pc	Russeil (2003 – table 6); see Table 4
	Warm ¹² CO cores	024°	2°	209 pc	Solomon et al (1985 – fig 1b); Bania (1980 – fig.7)

Scutum	^{12}CO at 8'	033°	0°	0 pc, at 5 kpc ⁽³⁾	Sanders et al (1985 – fig. 5b); see Table 3
	HII complex	032°	1°	87 pc	Russeil (2003 – Table 6); see Table 4
	^{26}Al	032°	1°	87 pc	Chen et al (1996 – fig.1)
	^{13}CO	032°	1°	87 pc	Stark & Lee (2006 – fig.1, $v = +95$ km/s)
	Thermal electron	032°	1°	87 pc	Taylor & Cordes (1993 – fig.4)
	Sync. 408 MHz	032°	1°	87 pc	Beuermann et al (1985 – fig.1)
	Dust 870 μm	031°	2°	174 pc	Beuther et al (2012 – fig.3)
	Dust 240 μm	031°	2°	174 pc	Drimmell (2000 – fig. 1)
	Warm ^{12}CO cores	030°	3°	262 pc	Solomon et al (1985 – fig. 1b)
	FIR [CII] & [NII]	030°	3°	262 pc	Steiman-Cameron et al (2010 – sect 2.1)
	HI atom	029°	4°	349 pc	Englmaier & Gerhard (1999 – table 1)
	Dust 2.4 μm	029°	4°	349 pc	Hayakawa et al (1981 – fig. 2a)
	Methanol masers	028°	5°	435 pc	Green et al (2011 – sect. 3.3.1); see Table 5
Dust 60 μm	026°	7°	609 pc	Bloemen et al (1990 – fig.5)	
Sagitarius	^{12}CO at 8'	051°	0°	0 pc, at 4 kpc ⁽³⁾	Cohen et al (1980 – fig.3); see Table 3
	HII complex	051°	0°	0 pc	Russeil et al (2007 – fig.4); see Table 4
	^{13}CO	051°	0°	0 pc	Stark & Lee (2006 – fig.1, $v = +60$ km/s)
	HI atom	050°	1°	70 pc	Englmaier & Gerhard (1999 – table 1)
	Dust 240 μm	050°	1°	70 pc	Drimmell (2000 – fig. 1)
	Methanol masers	050°	1°	70 pc	Reid et al (2014 – fig.1); see Table 5
	FIR [CII] & [NII]	050°	1°	70 pc	Steiman-Cameron et al (2010 – sect. 2.1)
	Warm ^{12}CO cores	049°	2°	140 pc	Solomon et al (1985 – fig. 1b)
	Dust 870 μm	049°	2°	140 pc	Beuther et al (2012 – fig.3)
	Thermal electron	049°	2°	140 pc	Taylor & Cordes (1993 – fig.4)
	Sync. 408 MHz	048°	3°	209 pc	Beuermann et al (1985 – fig. 1)
	^{26}Al	046°	5°	449 pc	Chen et al (1996 – fig.1)

Notes:

(1): Galactic longitude of arm tangent, as observed by each tracer (not theoretically computed).

(2): Angular distance from arm center, being positive towards arm's inner edge (towards Galactic Center), and negative in other direction (galactic anti-center).

(3): Linear separation from the arm center (^{12}CO), after converting the angular separation at the arm distance from the sun (taken from Figure 1 here); we assume 8.0 kpc for the distance of the Sun to the Galactic Center.

(4): When there are more than 2 published reports for a given arm tracer at a given spiral arm, then a separate table is provided in the Appendix.

Table 2 - The linear separation (S) from ^{12}CO of each arm tracer, in each spiral arm in the Milky Way⁽¹⁾

Chemical Tracer	S in Carina arm	S in Crux arm	S in Norma arm	S in Start of Per-Seus arm	S in Near 3-kpc arm	S in Scutum arm	S in Sagittarius arm	Mean separation	s.d.m. ⁽²⁾
	pc	pc	pc	pc	pc	pc	pc	pc	pc
^{12}CO at 8'	0	0	0	0	0	0	0	0	-(3)
HII complex	174	0	-366	-	105	87	0	0	78
^{13}CO	-	-	-	-	-	87	0	44	44
Thermal electron	87	0	0	-	-	87	140	63	27
^{26}Al	-	105	-366	-	-	87	449	69	167
HI atom	-	105	0	-	-	349	70	131	76
Synch. 408 MHz	-	105	0	279	-	87	209	136	93
FIR [CII] & [NII]	435	0	-	140	-	262	70	181	77
Warm ^{12}CO cores	-	-	-	-	209	262	140	204	35
Cold dust 240 μm	174	209	488	-	-	174	70	223	70 ⁽⁴⁾
Cold dust 870 μm	-	209	488	140	-	174	140	230	46 ⁽⁴⁾
Methanol masers	-	-	427	140	-	435	70	268	95
Hot dust 60 μm	262	209	122	419	-	609	-	324	86 ⁽⁵⁾
Hot dust 2.4 μm	-	-	488	279	-	349	-	372	61 ⁽⁵⁾

Notes:

(1): All data from Table 1 here.

(2): The s.d.m. in the last column is from the external scatter.

(3): There is a mean internal scatter of 42 pc, from the CO data in the Appendix (Table 3).

(4): Stats made on both cold dust tracers give a mean separation of 227 pc, with s.d.m. of 46 pc.

(5): Stats made on both hot dust tracers give a mean separation of 342 pc, with s.d.m. of 56 pc.

3. Arm tangent offset, for each tracer

Different arm tracers appear at slightly different galactic longitudes. To transfer angular to linear offsets, we used the canonical 4-arm logarithmic spiral model, with a Sun-Galactic Centre distance of 8.0 kpc, which is a mean of many recent measurements of this distance. The observed angular offset and computed linear separation of each individual arm tracer from the mid-arm are given, using the galactic longitude of the arm tangent for tracer X versus the galactic longitude of ^{12}CO arm tangent at low angular resolution.

Angle-wise, it can readily be seen in Table 1 that the hot dust arm tangents (and the methanol masers) are always inward, closer to the direction of the Galactic Center. Given enough arm tracers, and summing and averaging over all four spiral arms, one could determine if arm tracers have separate and parallel lanes in the Milky Way.

In **Table 2** we pull together the statistics over several spiral arms in the Milky Way, indicating the mean separation for each arm tracer, from the mid-arm. A net separation can be found for some of the arm tracers, notably for ^{12}CO (large beam), thermal electrons (galactic free electrons, from pulsar rotation measure and dispersion measure), relativistic electrons (408 MHz synchrotron), hot dust (60 μm and 2.4 μm together), and methanol masers (6.7 GHz). The ^{26}Al and HII complex tracers have large error bars, with a mean consistent with zero offset.

Here we make a short analysis of published stellar counts in the near infrared. The Glimpse program from the Spitzer Space Telescope has generated claims about alternating major and minor spiral arms (broad peaks in Fig.1 in Benjamin 2009; Fig. 14 and Fig.15 in Churchwell et al 2009), proposing the disappearance of the Sagittarius arm in stellar counts at $\lambda 4.5\mu\text{m}$; some authors have questioned their analysis. Steiman-Cameron (2010) and Steiman-Cameron et al (2010, Sect. 4.1) pointed out that the Sagittarius arm is observed in every major tracer, and that there is towards that galactic longitude an unusual high dust absorption, enhanced obscuration, and increased extinction (around the W51 complex). Not properly accounting for this extra dust could cause a decrease in star counts and the arm's disappearance. Also, the arm width of their major arm (Fig. 15 in Churchwell et al, 2009) is about 2.5 larger than that of their minor arm; this was questioned later. Vallée (2014a – Table 4) pointed out that the width of the Sagittarius arm is equal or nearly equal to that of the other arms, when using at least 4 different arm tracers.

4. Galactic arm cross-cut

4.1 Observational results

A crosscut of a spiral arm (**Figure 2**) shows the approximate position of a typical arm tracer with respect to the mid-arm, for the Milky Way. Many arms were used for the cross-cut. The direction to the Galactic Center is to the right. It is interesting that in Fig.2 the hot dust and methanol masers are always to the right of the ^{12}CO arm tangents, while the relativistic electron and free-free electron are always in between the mid-arm and the dust lane. There is no observed spiral arm tracer between the middle of the arm and the arm's outer edge, facing the outer Galaxy, except for stars (see Table 2).

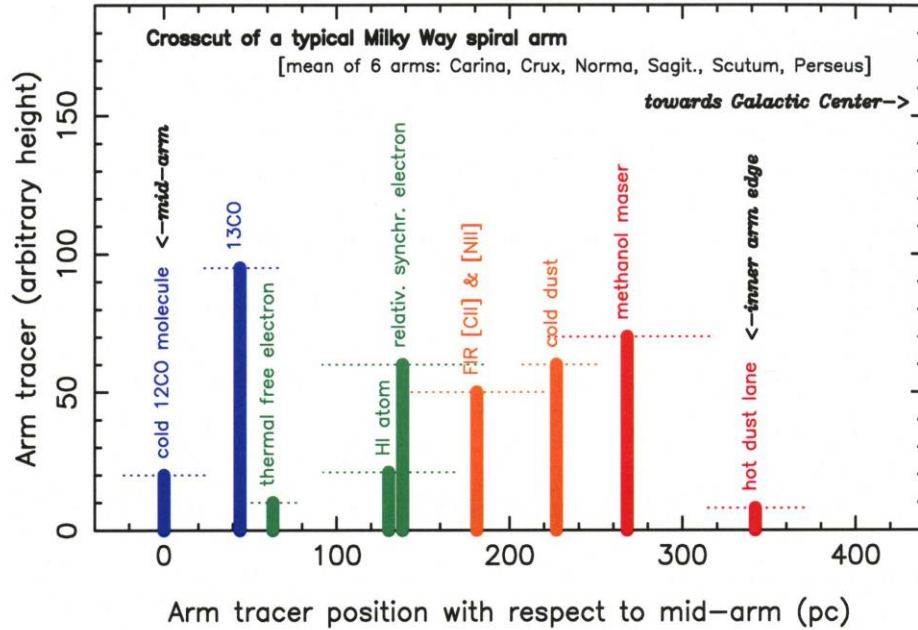


Figure 2. Average crosscut of various spiral arm in the Milky Way, showing where each different arm tracer appears. The sketch indicates the mean position of each spiral arm, as an offset from the mid-arm (^{12}CO tangent, at 0 pc) to the inner arm edge (hot dust tangent, near 340 pc). Vertical bars are arbitrary. The standard deviation of the mean (s.d.m.) is noted as an horizontal dotted line, for each arm tracer. Here the relativistic synchrotron is at 408 MHz. All data are from Table 2. For greater precision, the hot dust at 342 pc is an average over two wavelengths (2.4μ and 60μ); the cold dust at 227 pc is an average over two wavelengths (240μ and 870μ). For greater clarity, some tracers were omitted: the average HII complex at 0 pc, the ^{26}Al at 69 pc, and the warm CO cores at 204 pc.

The observed half width of a typical arm (near 340 pc from mid-arm to the inner edge) can be doubled in order to get the full arm width, giving about 680 pc. The standard deviation of the mean (s.d.m.) is given for each arm tracer with the horizontal dotted lines. The mean sdm observed for the arm tracers shown (including ^{12}CO) is near 80 pc (from **Table 2**), about only 12% of the full arm width.

The latest galactographic view of the Milky Way (**Figure 3**) shows the spiral arm lanes, using the data from Table 2 and Figure 2. On its way in a roughly circular orbit around the Galactic Center, the Sun would eventually reach the Perseus arm's hot dust lane first, and then later the next lanes (electrons; ...; CO) before exiting on the other arm's side.

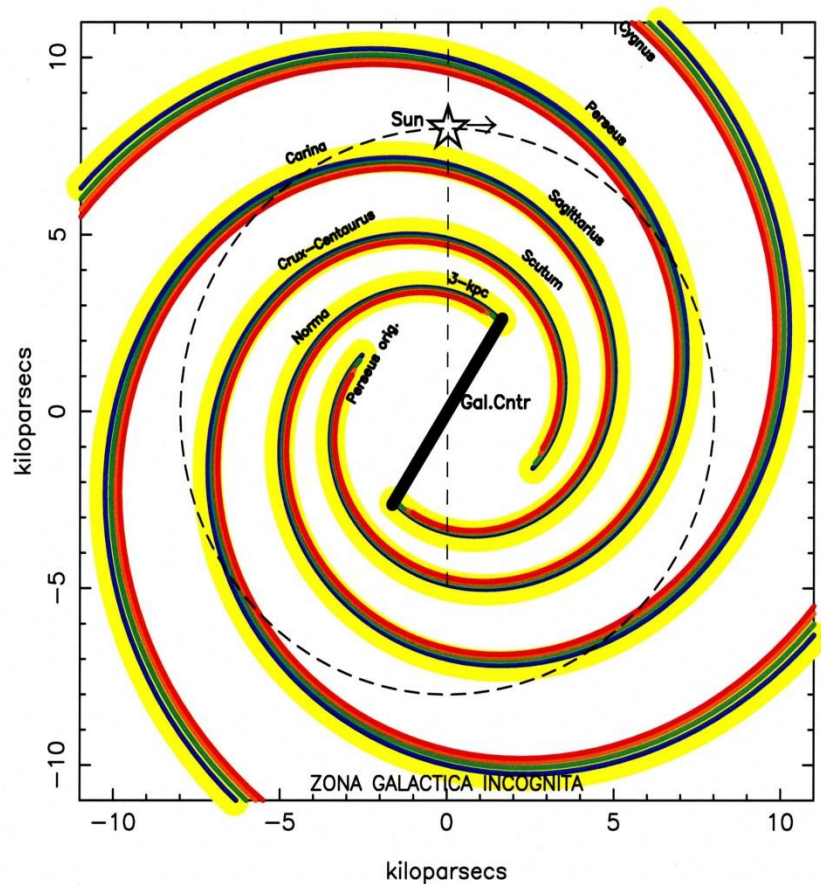


Figure 3. New galactography. Besides stars all over spiral arms, spiral arms harbor different components (tracers) at slightly at different (parallel) locations. Stars (yellow) are all over the arms. The ^{12}CO (and H_2) molecules peak near the middle of the arm (blue), while the hot dust (with masers and newborn stars) peak near the inner arm edge (red). Other intermediate tracers peak in between: thermal and relativistic electrons and HI atoms (green), and

cold dust with FIR cooling lines (orange). Same color coding used as in Figure 2. Updated from Vallée (2014a).

4.2 Comparisons with predictions from theories.

Here we make an attempt at some quick interpretation in terms of current spiral arm theories, basically trying to relate our results with their predictions. In this brief assessment of theories of spiral arms, we compare a few observed arm parameters: linear separation of different arm tracers from ^{12}CO (table 2), no arm tracer to the left of ^{12}CO (figure 2), the number of arms (4), average pitch angle (12°), arm shape (logarithmic) and arm spacing (equal), to first order – see Vallée (2014a).

The quasi-stationary density-wave theory can produce several arms. (i) The density wave theory predicts an orbital trajectory of the gas and stars going through spiral arms, and a linear separation between arm tracers as occasioned by a shocked gas and dust entering the arm from the inner edge, then some of it coalescing to form stars there (dust lane), progressing through the arm and exiting on the arm's outer edge (Roberts, 1975 – fig.3); this is similar to our orbit in Figure 1 here. (ii) In the density wave, the width of the dust lane (shocked lane) was predicted at 50 pc (e.g., Dobbs & Baba 2014, their sect. 3.5); this width is similar to our observed dust lane in Figure 2 here (with an error bar of 70 pc). (iii) In the density wave, the gas density maximum (at mid-arm) is separated from the shock lane by about 12 Myrs (Roberts, 1975 – Fig.2), or 306 pc for a gas velocity difference of 25 km/s (Dobbs & Baba 2014 – fig. 17b); this separation is similar to our observed arm's halfwidth of 360 pc (Table 2 here). Roberts (1975 – Fig.4) used a pitch angle near 10° , similar to that of the Milky Way. In the density-wave with 4 arms, the gas density maximum (potential minimum, broad CO at mid-arm) is also separated from the shock lane (hot dust) in the model of Gittins and Clarke (2004 – fig.16), and their 'standard model' has a low pitch angle of 5° (not the 12° found in the Milky Way). (iv) The density wave theory proposed that the peak of all tracers are between the inner edge of an arm and the mid-arm (as seen here in Table 2), excepting the stars distributed all over the arm. (v) The density wave predicts that the peak of the HII complex is located near the mid-arm (Roberts 1975 – fig.4, Gittins & Clarke 2004 – fig.16 far from the Galactic Center), as seen in Table 2 here.

There is a plethora of theories to generate spiral arms, in addition to the density-wave theory. (vi) The tidal theory involving a recent passage of the Sagittarius galaxy could induce two strong arms (Dobbs & Baba (2014, sect. 5.3), not four as found in the Milky Way. Of course, each of two Magellanic Clouds could perhaps produce its own set of twin arms. (vii) The bar-driven theory could induce two strong arms (Dobbs & Baba 2014 – sect.2.3), not four as found in the Milky Way. Of course, each of two straddling bars could perhaps produce its own set of twin arms. (viii) The stochastic, self-propagating star formation theory could produce a very irregular, flocculent arm pattern (Dobbs & Baba – sect. 2.5), not the quasi-regular pattern seen in the Milky Way. (ix) The swing-amplification theory could produce numerous flocculent arms irregularly located (Dobbs & Baba – sect. 5.2), not quasi-regularly spaced as for the Milky Way. (x) The transient-recurrent dynamic spiral theory (Dobbs & Baba 2014 – Sect. 2.2) has arms breaking and reconnecting, and high pitch angle between 20° and 40° (Dobbs & Baba 2014 – fig.10), unlike the low 12° as found generally in the Milky Way. (xi) The basic dynamo theory

does not predict any spiral arm as defined here (with dust and stars), contrary to observations, although it can produce magnetic arms – for a discussion, see Vallée (2011 – Sect. 9.7). In the presence of gaseous spiral arms, non-linear galactic dynamos predict that the interarm magnetic pitch angle will be compressed to roughly align with the gaseous arm pitch angle (Chamandy et al 2014 – sect. 7). (xii) The basic MHD theory, subjected to a spiral potential, predicts different pitch angle of the magnetic field (along the gas velocity) and that of the spiral arm (Dobbs & Price – fig.13); this is not at odd with some magnetic field observations – for a discussion, see Vallée (2011 – Sect.9.7.3).

In summary, the arm observations so far may be best compared to the density waves (i-v), but many other proposed theories could be partially contributing to the creation or maintenance over time of spiral arms or spurs (vi-xii). How much from each is unknown.

5. Conclusion

Our place in the Milky Way galaxy (Figure1), inside the flat galactic disk, makes it difficult to see the different spiral arms, being one behind another. Strong dust absorption in the disk does reduce our view at optical wavelengths. Still, radio, infrared and optical telescopes, equipped with spectrometers and other instruments, have allowed a picture to emerge with 4 long spiral arms where most of the gas and stars are positioned and their radial velocity measured. We presented here an updated and revised Catalogue of the mean data on the different spiral arm tracers (Table 1) and their accumulations (Table 3, Table 4, Table 5), covering 105 tracer entries.

We thus confirm here a separation between arm tracers (Table 2, Fig. 2), as claimed earlier by Vallée (2014a) with fewer tracers. In the Milky Way, each spiral arm tracer can occupy a parallel lane inside an arm – there is roughly 340 pc separation between the mid-arm (^{12}CO tracer lane) and the inner arm edge toward the Galactic Center (hot dust lane). This provides us a fascinating view of the inside of a typical spiral arm in the Milky Way galaxy, despite the Sun's awkward position inside the flat galactic disk (Figure 3). Our interpretation in terms of the many proposed spiral arm theories is still sketchy (section 4.2), while currently favoring the hunt for the density waves.

Acknowledgements.

The figure production made use of the PGPLOT software at the NRC-nsip in Victoria. I thank a referee for insightful and helpful comments, which helped to correct and improve the clarity of the text.

Appendix A.

Here are some of the published individual tracer values, when there is more than one for each tracer in each spiral arm.

Table 3 lists numerous individual CO entries (not earlier than 1980).

Table 4 provides individual HII complex entries (not earlier than 1980).

Table 5 gives individual maser entries (not earlier than 1980).

Table 3 - Published CO J=1-0 results at low angular resolution (since 1980)

Arm name	Tangent Longitude	Telescope HPBW and survey name	Reference
Carina	280°	8.8' Columbia	Alvarez et al (1990 – table 4)
	280°	8.8' Columbia	Grabelsky et al (1987 – sect. 3.1.2)
	281°	8.8' Columbia	Grabelsky et al (1988 – fig.4)
	282°	8.8' Columbia	Bronfman et al (2000b – table 2)
	283°	8.8' Columbia	Bronfman et al (2000a – Section 3.4)
	281.2 ±1.3	mean and r.m.s.	s.d.m of 0.6°, worth 51 pc at 5 kpc
Crux-Cen-Taurus	308°	8.8' Columbia	Bronfman et al (2000a – sect. 3.4)
	308°	8.8' Columbia	Bronfman (2008 – sect. 4)
	309°	8.4' CfA	Dame & Thaddeus (2011 – fig.4)
	309°	8.8' Columbia	Bronfman et al (2000b – table 2)
	310°	8.8' Columbia	Alvarez et al (1990 – table 4)
	310°	8.8' Columbia	Bronfman et al (1988 – fig. 7)
	310°	8.8' Columbia	Bronfman et al (1989 – sect. 4)
	310°	8.8' Columbia	García et al (2014 – table 3)
	309.3 ±0.9	mean and r.m.s.	s.d.m of 0.3°, worth 34 pc at 6 kpc
Norma	328°	8.8' Columbia	Alvarez et al (1990 – table 4)
	328°	8.8' Columbia	Bronfman et al (1988 – fig. 7)
	328°	8.8' Columbia	Bronfman et al (1989 – sect. 4)
	328°	8.8' Columbia	Bronfman (1992 – fig.6)
	328°	8.8' Columbia	Bronfman et al (2000a – sect. 3.4)
	328°	8.8' Columbia	Bronfman et al (2000b – table 2)
	328°	8.8' Columbia	Bronfman (2008 - sect. 4)
	330°	8.8' Columbia	García et al (2014 – table 3)
	330°	8.8' Columbia	Grabelsky et al (1987 – sect. 3.1.2)
	328.4 ±0.9	mean and r.m.s.	s.d.m of 0.4°, worth 37 pc at 7 kpc
Start of Perseus	336°	8.8' Columbia	Bronfman et al (1989 – sect. 4)
	336°	8.8' Columbia	Bronfman (2008 – sect. 4)
	337°	8.8' Columbia	Alvarez et al (1990 – table 4)
	337°	8.8' Columbia	Bronfman et al (2000a – sect. 3.4)
	337°	8.8' Columbia	Bronfman et al (2000b - table 2)
	337°	8.8' Columbia	Dame & Thaddeus (2008 – sect. 1)
	338°	8.8' Columbia	García et al (2014 – table 3)

	336.9 ±0.7	mean and r.m.s.		s.d.m of 0.3°, worth 37 pc at 8 kpc
Near 3-kpc arm	026°	7.5'	Columbia	Cohen et al (1980 – fig.3)
	026°	7.5'	Columbia	Dame et al (1986 – fig.9)
	026°		mean	
Scutum	031°	8.4'	CfA	Dame & Thaddeus (2011 – fig.4)
	033°	1.1'	NRAO	Sanders et al (1985 – fig.5b)
	034°	7.5'	Columbia	Cohen et al (1980 – fig.3)
	035°	1.0'	Texas	Chiar et al (1994 – Sect. 3)
	033.2 ±1.7	mean and r.m.s.		s.d.m of 0.8°, worth 70 pc at 5 kpc
Sagittarius	051°	7.5'	Columbia	Cohen et al (1980 – fig.3)
	051°	7.5'	Columbia	Dame et al (1986 – fig.9)
	051°		mean	

Table 4 – Published HII complex results

Arm name	Tangent longitude	Range	Reference
Carina	284°	optical	Russeil (2003 – table 6)
	284°	radio	Downes et al (1980 – fig.4)
	284°	mean	
Crux-Centaurus	309°	optical	Russeil (2003 – table 6)
	309°	radio	Downes et al (1980 – fig.4)
	309°	mean	
Norma	323°	optical	Russeil (2003 – table 6)
	328°	radio	Downes et al (1980 – fig.4)
	325.5 ±3.5°	mean and r.m.s.	
Near 3-kpc arm	025°	optical	Russeil (2003 – table 6)
	025°	radio	Sanders et al (1985 – fig. 5a)
	025°	mean	
Scutum	032°	optical	Russeil (2003 – table 6)
	031°	radio	Downes et al (1980 – fig.4)
	031.5° ±0.7°	mean and r.m.s.	
Sagittarius	056°	optical	Russeil (2003 – table 6)
	051°	optical	Russeil et al (2007 – fig.4)
	046°	radio	Downes et al (1980 – fig.4)
	051.0° ±5.0°	mean and r.m.s.	

Table 5 – Published maser results

Arm name	Tangent longitude	Range	Reference
Norma	331.5°	methanol	Caswell et al (2011 – Sect. 4.6.2)
	331.5°	mean	
Start of Perseus	338°	methanol	Green et al (2011 – sect. 3.3.1)
	338°	methanol	Green et al (2012 – Sect.2)
	338.0°	mean	
Scutum	026°	methanol	Green et al (2011 – sect. 3.3.1)
	026°	methanol	Green et al (2012 – Sect.2)
	030°	methanol, water	Reid et al (2014 – fig.1)
	031°	methanol, water	Sato et al (2014 – fig3)
	028.2° ±2.6°	mean and r.m.s.	
Sagittarius	049.6°	methanol	Pandian & Goldsmith (2007 – sect.4)
	050°	methanol, water	Reid et al (2014 – fig.1)
	051°	methanol, water	Wu et al (2014 – sect. 4.2)
	050.2° ±0.7°	mean and r.m.s.	

References:

- Alvarez, H. May, J., Bronfman, L., "The rotation of the Galaxy within the solar circle", 1990, *Astrophys. J.*, v348, p495-502.
- Bania, T.M., "Carbon Monoxide in the inner Galaxy: the 3-kpc arm and other expanding features", 1980, *ApJ*, v242, p95-111.
- Benjamin, R.A., "Spiral arm tangencies in the Milky Way", 2009, *Proc. IAU Symp.*, v254, p319-322.
- Beuermann, K., Kanbach, G., Berkhuijsen, E.M., "Radio structure of the Galaxy – Thick disk and thin disk at 408 MHz", 1985, *A&A*, v153, p17-34.
- Beuther, H., Tackenberg, J., Linz, H., Henning, Th., Schuller, F., Wyrowski, F., Schilke, P., Menten, K., Robitaille, T.P., Wlamsley, C.M., Bronfman, L., Motte, F., Nguyen-Luong, Q., Bontemps, S., "Galactic structure based on the Atlasgal 870 μm survey", 2012, *ApJ*, v747, a43, p1-8.
- Bloemen, J.B., Deul, E.R., Thaddeus, P., "Decomposition of the FIR Milky Way observed by IRAS", 1990, *A&A*, v233, p437-455.
- Bronfman, L., "Molecular clouds and young massive stars in the Galactic disk", 1992, *Astrophys Space Sci Lib.*, v180, p131-154.
- Bronfman, L. "Massive star formation in the southern Milky Way", 2008, *Ap Sp Sci.*, v313, p81-85.
- Bronfman, L., Alvarez, H., Cohen, R.S., Thaddeus, P., "A deep CO survey of molecular clouds in the southern Milky Way", 1989, *ApJ Suppl Ser.*, v71, p481-548.
- Bronfman, L., Casassus, S., May, J., Nyman, L.-A., "The radial distribution of OB star formation in the Galaxy", 2000a, *Astron. & Astrophys.*, v358, p521-534.
- Bronfman, L., Cohen, R.S., Alvarez, H., May, J., Thaddeus, P., "A CO survey of the southern Milky Way: the mean radial distribution of molecular clouds within the solar circle", 1988, *ApJ*, v324, p248-266.
- Bronfman, L., May, J., Luna, A., "A CO survey of the southern Galaxy", 2000b, *ASP Confer. Ser.*, v217, p66-71.
- Caswell, J.L., Fuller, G.A., Green, J.A., Avison, A., Breen, S.L., Ellingsen, S.P., Gray, M.D., Pestalozzi, M.R., Quinn, L., Thompson, M.A., Voronkov, M.A., "The 6GHz methanol multibeam maser catalogue – III. Galactic longitudes 330° to 345°", 2011, *MNRAS*, v417, p1964-1995.
- Chamandy, L., Shukurov, A., Subramanian, K., Stoker, K., "Non-linear galactic dynamos : a toolbox", 2014, *MNRAS*, v443, p1867-1880.
- Chen, W., Gehrels, N., Diehl, R., Hartmann, D., "On the spiral arm interpretation of Comptel ^{26}Al map features", 1996, *A&A Suppl.*, v120, p315.
- Chiar, J.E., Kutner, M.L., Verter, F., Leous, J., "A comparison of CO (J=1-0) and CO (J=2-1) emission in the Milky Way molecular ring", 1994, *ApJ*, v431, p658-673.

Churchwell, E., Babler, L.B., Meade, M.R., Whitney, B.A., Benjamin, R., Indebetouw, R., Cyganowski, C., Robitaille, T.P., Povich, M., Watson, C., Bracker, S., "The Spitzer/GLIMPSE surveys: a new view of the Milky Way", 2009, Publ. Astron. Soc. Pacific, v121, p213-230.

Cohen, R.S., Cong, H., Dame, T.M., Thaddeus, P., "Molecular clouds and galactic spiral structure", 1980, ApJ, v239, L53-L56.

Dame, T.M., Elmegreen, B.G., Cohen, R.S., Thaddeus, P., "The largest molecular cloud complexes in the first galactic quadrant", 1986, ApJ, v305, p892-908.

Dame, T.M., Thaddeus, P., "A new spiral arm of the Galaxy: the Far 3kpc arm", 2008, ApJ, v683, L143-L146.

Dame, T.M., Thaddeus, P., "A molecular spiral arm in the far outer galaxy", 2011, ApJL, v734, L24, p1-4.

Dobbs, C., Baba, J., "Dawes review 4 : spiral structures in disc galaxies", 2014, Publ Astron Soc Australia, in press – astro-ph.GA arXiv:1407.5062

Dobbs, C.L., A. Burkert, "The myth of the molecular ring", 2012, Monthly Notices Royal Astronomical Society, v421, p2940-2946.

Dobbs, C.L., Price, D.J., "Magnetic fields and the dynamics of spiral galaxies", 2008, MNRAS, v383, p497-512.

Downes, D., Wilson, T.L., Bieging, J., Wink, J., "H110 α and H₂CO survey of galactic radio sources", 1980, A&A Suppl., v40, p379-394.

Drimmel, R., "Evidence for a 2-armed spiral in the Milky Way", 2000, A&A, v358, L13-L16.

Englmaier, P., Gerhard, O., "Gas dynamics and large-scale morphology of the Milky Way galaxy", 1999, MNRAS, v304, p512-534.

García, P., Bronfman, L., Nyman, L.-A., Dame, T.M., Luna, A., "Giant molecular clouds and massive star formation in the southern Milky Way", 2014, AstrophysJSuppl.Ser., v212, a2, p1-33.

Gittins, D.M., Clarke, C.J., "Constraining corotation from shocks in tightly wound spiral galaxies", 2004, MNRAS, v349, p909-921.

Grabelsky, D.A., Cohen, R.S., Bronfman, L., Thaddeus, P., May, J., "Molecular clouds in the Carina arm – largescale properties of molecular gas and comparison with HI", 1987, Astrophysical journal, v315, p122-141.

Grabelsky, D.A., R.S. Cohen, L. Bronfman, P. Thaddeus, "Molecular clouds in the Carina arm – the largest objects, associated regions of star formation, and the Carina arm in the Galaxy", 1988, Astrophysical journal, v331, p181-196.

Green, J.A., Caswell, J.L., McClure-Griffiths, N.M., Avison, A., Breen, S.L., Burton, M.G., Ellingsen, S.P., Fuller, G.A., Gray, M.D., Pestalozzi, M., Thompson, M.A., Voronkov, M.A., "Major structures of the inner Galaxy delineated by 6.7GHz methanol masers", 2011, ApJ, v733, a27, p1-17.

Green, J.A., Caswell, J.L., McClure-Griffiths, N.M., Avison, A., Breen, S.L., Burton, M.G., Ellingsen, S.P., Fuller, G.A., Gray, M.D., Pestalozzi, M., Thompson, M.A., Voronkov, M.A., "Tracing major structures of the inner Galaxy with 6.7GHz methanol masers", 2012, EPJ Web of conferences, v19, a06007, p1-3.

Hayakawa, S., Matsumoto, T., Murakami, H., Uyama, K., Thomas, J.A., Yamagami, T., "Distribution of near infrared sources in the galactic disk", 1981, A&A, v100, p116.

Heiles, C., Haverkorn, M., "Magnetic fields in the multiphase interstellar medium", 2012, Space Sci Rev., v166, p293-305.

Martinez-Valpuesta, I., "A bar/bulge model for the Milky Way", 2013, in Highlights of Spanish Astrophysics VII, Proc. of the X Sci. Mtg, of the SEA, ed. by Guirado, J.C., Lara, L.M., Quilis, V., Gorgas, J. (Sociedad Espanola de Astronomia, Barcelona, Spain), p484-491.

Pandian, J.D., Goldsmith, P.E., "The Arecibo methanol maser galactic plane survey. II. Statistical and multiwavelength counterpart analysis", 2007, ApJ, v669, p435-445.

Reid, M.J., Menten, K.M., Brunthaler, A., Zheng, X.W., Dame, T.M., Xu, Y., Wu, Y., Zhang, B., and 8 others, "Trigonometric parallaxes of high mass star forming regions: the structure and kinematics of the Milky Way", 2014, ApJ, v783, a130, p1-14.

Roberts, W.W., "Theoretical aspects of galactic research", 1975, Vistas in Astron., v19, p91-109.

Romero-Gómez, M., Antoja, T., Figueras, F., Aguilar, L.A., Athanassoula, E., "The invariant manifolds and the Milky Way galactic bar(s)", 2013, in Highlights of Spanish Astrophysics VII, Proc. of the X Sci. Mtg, of the SEA, ed. by Guirado, J.C., Lara, L.M., Quilis, V., Gorgas, J. (Sociedad Espanola de Astronomia, Barcelona, Spain), p618-622.

Russeil, D., "Star-forming complexes and the spiral structure of our Galaxy", 2003, A&A, v397, p133-146.

Russeil, D., Adami, C., Georgelin, Y.M., "Revised distances of Northern HII regions", 2007, A&A, v470, p161-171.

Sanders, D.B., Scoville, N.Z., Solomon, P.M., "Giant molecular clouds in the Galaxy. II. Characteristics of discrete features", 1985, ApJ, v289, p373-387.

Sato, M., Wu, Y.W., Immer, K., Zhang, B., Sanna, A., Reid, M.J., Dame, T.M., Brunthaler, A., Menten, K.M., "Trigonometric parallaxes of star forming regions in the Scutum spiral arms", 2014, ApJ, v793, a72, p1-15.

Solomon, P.M., Sanders, D.B., Rivolo, A.R., "The Massachusetts-Stony-Brook galactic plane CO survey: disk and spiral arm molecular cloud populations", 1985, ApJ, v292, L19-L24.

Stark, A.A., Lee, Y., "Giant molecular clouds are more concentrated toward spiral arms than smaller clouds", 2006, ApJ, v641, L113-L116.

Steiman-Cameron, T.Y., "Twin masks of spiral structure? A local perspective", in Galaxies and their masks, ed. by Block, D.L., Freeman, K.C., Puerari, I., Springer, 2010, p45-58.

Steiman-Cameron, T.Y., Wolfire, M., Hollenbach, D., "COBE and the galactic interstellar medium: geometry of the spiral arms from FIR cooling lines", 2010, ApJ, v722, p1460-1473.

Taylor, J.H., Cordes, J.M., "Pulsar distances and the galactic distribution of free electron", 1993, ApJ, v411, p674-684.

Vallée, J.P., "The Milky Way's Spiral Arms Traced by Magnetic Fields, Dust, Gas, and Stars", 1995, ApJ, v454, p119-124.

Vallée, J.P., « Metastudy of the Spiral Structure of Our Home Galaxy », 2002, ApJ, v566, p261-266.

Vallée, J.P., « The Spiral Arms and Interarm Separation of the Milky Way: An Updated Statistical Study », 2005, AJ, v130, p569-575.

Vallée, J.P., « New Velocimetry and Revised Cartography of the Spiral Arms in the Milky Way—A Consistent Symbiosis », 2008, AJ, v135, p1301-1310.

Vallée, J.P., “Magnetic field in the Galactic Universe, as observed in supershells, galaxies, intergalactic and cosmic realms”, 2011, New Astron Rev., v55, p91-154.

Vallée, J.P., “Magnetic Milky Way”, 2012, Europ. Astron. Soc. Publ. Ser., v56, p81-86.

Vallée, J.P., “A synthesis of fundamental parameters of spiral arms, based on recent observations in the Milky Way”, 2013, IJAA, v3, p20-28.

Vallée, J.P., “The spiral arms of the Milky Way: the relative location of each different arm tracer, within a typical spiral arm width”, 2014a, Astron.J., v.148, a5, p1-9.

Vallée, J.P., “On a persistent large discrepancy in some observed parameters of the spiral arm in the Milky Way – a statistical and modelling analysis”, 2014b, MNRAS, v442, p2993-2998.

Wu, Y.W., Sato, M., Reid, M.J., Moscadelli, L., Zhang, B., Xu, Y., Brunthaler, A., Menten, K.M., Dame, T.M., Zheng, X.W., “Trigonometric parallaxes of star forming regions in the Sagittarius spiral arm”, 2014, A&A, v566, a17, p1-26.